Available online at www.sciencedirect.com
SCIENCE DIRECT®
Physica E 25 (2004) 326–334
PHYSICA E
www.elsevier.com/locate/physe

Electronic skin: architecture and components

Sigurd Wagner[a,*], Stéphanie P. Lacour[a], Joyelle Jones[a], Pai-hui I. Hsu[a], James C. Sturm[a], Teng Li[b], Zhigang Suo[b]

[a] *Department of Electrical Engineering and PRISM, Princeton University, Princeton, NJ 08544, USA*
[b] *Division of Engineering and Applied Sciences, Harvard University, Cambridge, MA 02139, USA*

Available online 28 July 2004

Abstract

Conceptual hardware architecture of skin-like circuits is described. An elastomeric skin carries rigid islands on which active subcircuits are made. The subcircuit islands are interconnected by stretchable metallization. We concentrate on recent advances in stretchable thin-film conductors, by covering their construction, evaluation, and laboratory and theoretical analysis. Reversibly stretchable conductors with electrically-critical strains ranging from 10% to 100% have been made.

PACS: 73.61. A; 81.05. B; 81.05. L; 81.40. J; 81.70. B

Keywords: Stretchable metal film; Large-area electronics; Macroelectronics; Elastomer

1. Introduction

Sensor skin [1], electronic muscles [2], electrotextiles [3], and conformal displays [4] represent a new kind of integrated electronics that is large area and shapeable. The commercial success of flat panel displays, the most visible example of large area electronics, has given credibility to these very advanced concepts. Large area and flexible electronics may range from the add-on hybrid of an i-pod embedded in a jacket to the fully integrated textile circuit woven from component fibers [5]. Electronic skins for robots and medical prostheses—multifunctional structures, in which sensors and actuators are closely integrated with microelectronic circuits—bring a new dimension to electronics flexibility. Shaped electronics and skin-like electronics may experience large deformation strains. A disk detector array may see its surface area double to be shaped as a hemispherical detector array. When wrapped over elbow-like joints, the skin may be stretched and relaxed many times by $\sim 15\%$.

Semiconductor integrated circuits and MEMS technology use rigid and stiff substrates that are not adapted to flexible structures, and thin active device materials that fracture at a critical strain of $\sim 1\%$ [6]. Free-standing thin metal films also break under tensile strain of the order of 1% [7,8].

*Corresponding author. Tel.: +1-609-258-4631; fax: +1-609-258-6279.
E-mail address: wagner@princeton.edu (S. Wagner).

1386-9477/$ - see front matter
doi:10.1016/j.physe.2004.06.032

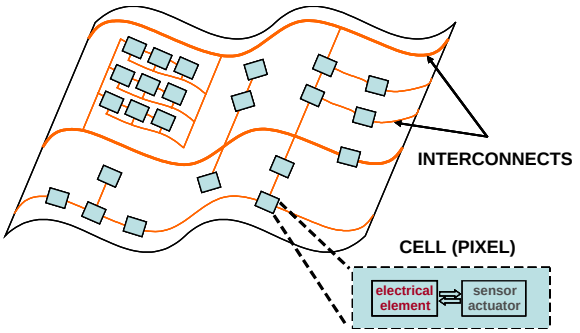

Fig. 1. Concept of a conformable electronic surface made on stretchable substrate. A cell that contains the electro-mechanical function is replicated many times. The cells are interconnected with flexible and stretchable metallization.

To achieve flexible and stretchable skin, subcircuit cells, made of a transducer and an electronic circuit, will be placed on mechanically separated islands, which are fabricated on a deformable substrate that takes up most of the total strain [4]. Fig. 1 is a sketch of such an island-carrying electronic surface. The islands are made sufficiently rigid to protect them from breaking when the circuit is deformed one time or by repeated stretching. The subcircuits are electrically connected with stretchable metal conductors. We know three options for making deformable interconnects: making thin metal films that can withstand large plastic deformation [9,10], deforming a sacrificial mask that then serves in lift-off metallization [4,11], and making stretchable metallization. The latter approach is the subject of this paper.

2. Stretchable metallization

Initially our approach of stretchable metallization was to build metal waves that can be stretched flat reversibly. Complex wave patterns of thin metal film on compliant substrates such as polydimethylsiloxane (PDMS) have been the subject of recent research [12–17]. Stress that may develop in a metal film during its deposition [18,19] on elastomeric substrates is released by random buckling [12] or waves [13,14,20]. The stress within the thin metal film/elastomer structure sets up the wave pattern. We have modelled these structures with the results shown in Eqs. (1) and (2) [20].

$$\frac{2\pi h}{\lambda} = \left(\frac{4(1-\nu_1)^2 E_2}{E_1}\right)^{1/3}, \tag{1}$$

$$\frac{A}{h} = \sqrt{\frac{2}{3}}\sqrt{\frac{\varepsilon_0}{\varepsilon_c} - 1}. \tag{2}$$

The wavelength λ depends on the Au film thickness h, the Young's moduli E_1 and E_2 and the Poisson ratios ν_1 and $\nu_2 = 0.5$, of the metal and the elastic substrate. The amplitude A depends on the initial built-in strain ε_0 and the critical buckling strain of the film ε_c. ε_0 is produced by the built-in stress, which depends on film deposition. ε_c is the buckling threshold. When $|\varepsilon_0| < |\varepsilon_c|$ the film remains flat. ε_c depends on mechanical parameters and geometry.

We have discovered that built-in wavy gold films on PDMS membranes can be stretched far more than free-standing gold films, yet remain electrically conducting [14,15]. Furthermore their stretchability can be improved when controlling the buckles' orientation, amplitude, and wavelength. To do so, thin film coatings are deposited on uni-axially pre-stretched rubber-like substrates [16,17,20,21]. Upon release of the pre-stretched substrate, a controlled sinusoidal surface pattern forms in the film/substrate structure [16,17,21,22]. The length of the thin film, when stretched flat, is given by Eq. 3 [20]:

$$L_{\max} = 2N \times \int_0^{\pi} \sqrt{1 + \left(\frac{2\pi A}{\lambda}\cos\frac{2\pi x}{\lambda}\right)^2}\,\mathrm{d}x, \tag{3}$$

where N is the number of waves along the sample length.

We have shown that such structures (gold films on pre-stretched PDMS membranes) can be stretched far beyond this flat condition, yet remain electrically conducting [14, 20–23]. The reason is that the mechanical fracture hence electrical failure of a thin metal film is suppressed or delayed when the film is bonded strongly to a compliant substrate [10].

Therefore, to make a metal film stretchable it can be deposited either on a pre-stretched substrate; or a relaxed elastomeric substrate.

In this paper, we describe the fabrication process, topography and microstructure of conductors both on relaxed and pre-stretched substrates, show their electrical resistance as a function of the applied mechanical strain, and briefly survey ongoing theoretical studies of the mechanics of metal films bonded to polymer substrates.

3. Experiments

3.1. Sample preparation

The substrate is a 1-mm thick membrane of poly dimethyl siloxane (PDMS) prepared by casting in a plastic Petri dish. A curing agent and PDMS prepolymer (Dow Corning, Sylgard 184) are thoroughly mixed in a 1:10 weight ratio. After degassing, the polymer mixture is poured in the dish and cured at 60°C for several hours. No surface treatment is performed before the metal deposition.

Electron-beam evaporation is used to deposit the thin metal layers onto the elastomeric substrate. Chromium (Cr) and gold (Au) are evaporated successively in the vacuum chamber with sample rotation. The sample temperature does not exceed 60°C during the process. The 5-nm thick chromium layer ensures the Au adhesion on the PDMS substrate. 5- to 500-nm thick gold layers are deposited at a constant evaporation rate of ~ 2 Å/s.

3.1.1. Relaxed substrates

The metal on relaxed PDMS substrates is patterned using a shadow mask made of polyimide foil (Dupont, Kapton E). The flexible polyimide shadow mask provides an easy and dry technique to pattern thin metal layers. The Kapton mask is made to adhere to the PDMS membrane prior to metal evaporation. All conductors are 1-in (2.54 cm) long. Their width W varies from 0.2 to 2-mm. After the evaporations, the Kapton foil is peeled off the PDMS surface.

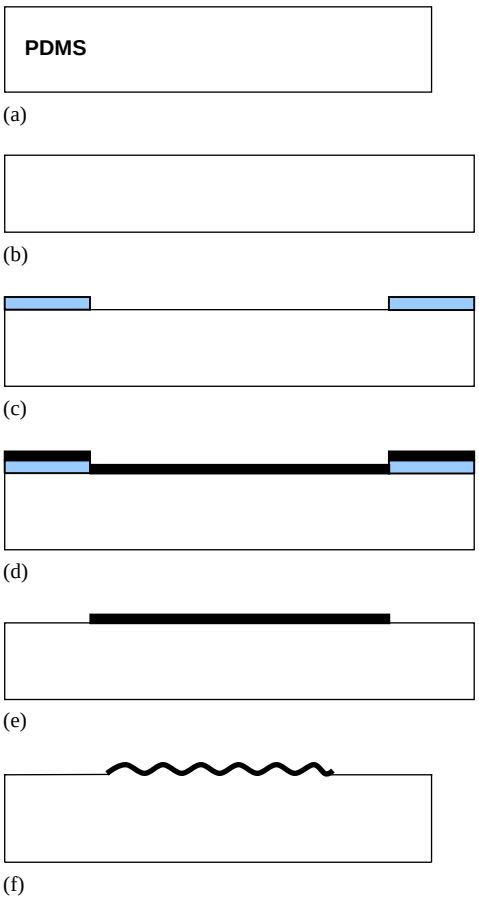

Fig. 2. Fabrication steps for gold interconnects on a pre-stretched elastomeric PDMS substrate. (a) as-prepared PDMS substrate; (b) pre-stretched PDMS; (c) laminated Riston photo-resist mask; (d) evaporated metal films; (e) lift-off; (f) release from pre-stretch; the gold stripe buckles.

3.1.2. Pre-stretched substrates

The substrate length is L_0 when relaxed (Fig. 2a), and L_{max} when stretched (Fig. 2b). A home-made fixture holds the substrate to a pre-stretch strain, $(L_{max} - L_0)/L_0$, of between 10% and 20% [21]. Stripes are patterned on the substrate by lift-off using Dupont Riston photo-resist. The UV-exposed and developed Riston film is laminated onto the pre-stretched PDMS membrane prior to metal evaporation (Fig. 2c). Subsequently, a 5-nm thick chromium adhesion layer and a 25-nm thick gold layer are electron-beam evaporated on the PDMS substrate (Fig. 2d). The Riston is stripped in a KOH solution (Fig. 2e). When the PDMS

substrate is released from its holder, the metal stripes form waves (Fig. 2f). Before release from an elongation of 15%, the Au stripes are 500-μm wide and 4.6-mm long.

3.2. Evaluation techniques

Electro-mechanical properties are evaluated in a home-made tensile tester where the sample is clamped at both ends [23]. We measure the electrical resistance with a Keithley 4140 source-meter, the elongation with the stepper motor position, the surface topography with a CCD camera microscope, and the force with a load cell. In typical tests the tensile strain is raised in steps of 0.1–0.5% every half-minute or minute. The electrical resistance is recorded every 2–10 s, and pictures are taken during the test.

The sample surface is characterized using optical microscopy and scanning electron microscopy (SEM). To avoid charging, a 1.5-nm thick layer of iridium is sputtered onto each sample prior to SEM imaging.

4. Experimental results

4.1. Surface topography

We obtained two kinds of topography. Evaporation on relaxed PDMS substrates produces either wavy (buckled) or flat gold stripes. Gold conductors made by evaporation on pre-stretched samples are always wavy upon release of the pre-stretch.

4.1.1. Gold evaporated on relaxed substrates

Under the optical microscope all gold layers are shiny and continuous. Surprisingly, we observe two sample topographies, regardless of gold stripe thickness and width. As shown in Fig. 3, the sample surface can be buckled (Fig. 3a) or flat (Fig. 3b).

Stress built into the gold film during its evaporation [18,19] induces the film to buckle [20,23], as shown in Fig. 3a. When the metal is deposited in stripes of width <1 mm, ordered parallel waves form in the Au layer [14]. The wave amplitude is smaller than 0.5 μm. The wavelength increases with the Au film thickness as described by Eqs. (1) and (2) [20]. Samples with the smooth surface of Fig. 3b exhibit no waviness. The difference in topography shown in Fig. 3 may result from compressive (Fig. 3a) and tensile stress (Fig. 3b) built into the metal film. Sample microstructure supports this hypothesis (the difference in electrical resistance is a consequence of the microstructure).

The SEM micrographs shown in Fig. 4 illustrate differences in the microstructure of the samples. Initially buckled samples are continuous (Fig. 4a), and have a surface grain size that increases from $\sim$15-nm for 25-nm thick films to $\sim$35-nm for 200-nm thick films. Flat samples present a network of randomly arranged micro-cracks (Fig. 4b) which are micrometer size, Y-shaped, not connected to each other, and apparently occur at grain boundaries. The shape and distribution of the cracks do not depend on the Au thickness. While the two types of film suggest the effects of compressive and tensile stresses, to date we have

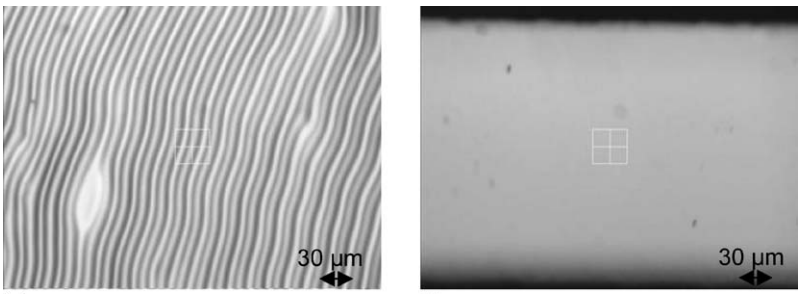

(a) (b)

Fig. 3. Optical microscope/CCD camera photographs of 50-nm thick gold layers evaporated on 1-mm thick silicone membrane. After evaporation the sample may be (a) buckled or (b) flat. Both pictures are $340 \times 250\,\mu m^2$. The stripe direction is from left to right.

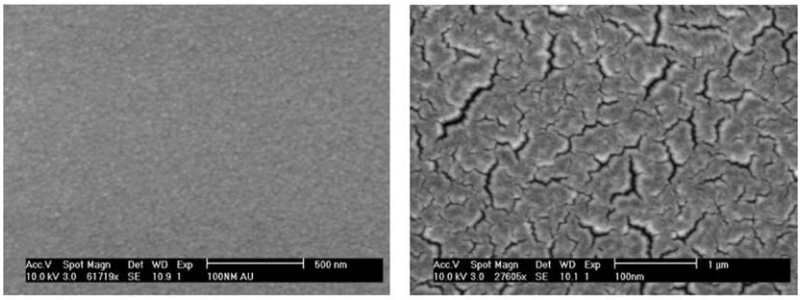

Fig. 4. SEM micrographs of 100-nm thick gold layers. The sample on the left is macroscopically buckled and that on the right is flat. (a) The buckled sample is continuous and has a grain-like structure, whereas (b) the flat sample surface presents a network of randomly arranged micro-cracks.

found no obvious correlation between the Au film thickness and geometry, and the microstructure.

4.1.2. Pre-stretched substrates

Upon substrate release, the PDMS membrane contracts in the X—its length—direction and expands in the Y—its width—direction. This puts the metal film into compressive stress in the X direction, and it buckles to a wave in the X direction. The tensile stress in the Y direction produces cracks in the metal film, normal to the Y direction. These cracks are evident at 1% and 15% strain in the photographs of Fig. 5. Judging from the spacing between the cracks, we expect that gold stripes of width less than $\sim 50\,\mu m$ will not form such cracks.

Fig. 6 shows the 3-D profile of a gold film after the substrate is released. The film was continuous, and formed a wave in the pre-stretch direction, X. The wavelength was $\lambda \approx 8.4\,\mu m$ and the amplitude $A \approx 1.2\,\mu m$. The built-in strain ε_0 calculated from the length of the sine wave trace λ_{trace}, as $\varepsilon_0 = (\lambda_{trace} - \lambda)/\lambda$, was $\sim 10.5\%$. ε_0 was smaller than the design pre-stretch, $(L_{max} - L_0)/L_0$ of 15%. We ascribe the difference between design and actual strain to film-substrate interactions, which have been observed earlier [12,21,23] but are not yet understood.

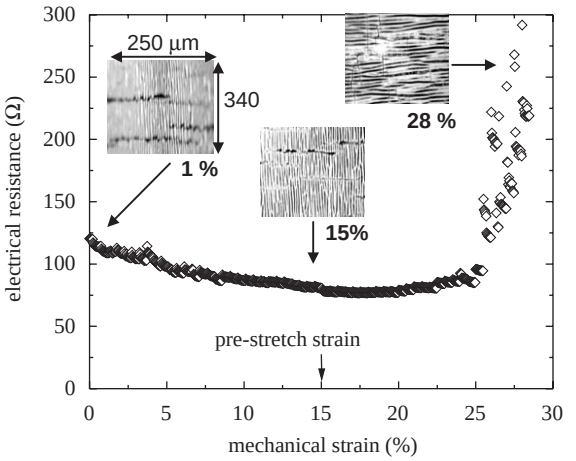

Fig. 5. Variation of the electrical resistance R with applied tensile strain ε of a 500-μm wide, 25-nm thick, gold stripe made on a substrate pre-stretched by 15%. Direction of stretching in the photographs is horizontal.

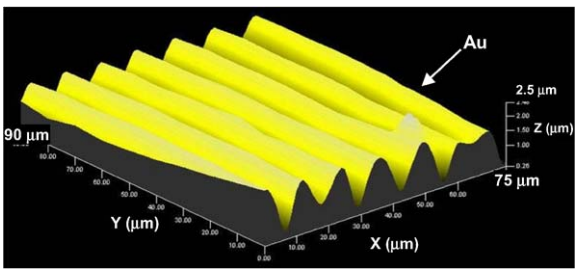

Fig. 6. 3D profile of a Au surface wave after release from 15% pre-stretch.

4.2. Electrical resistance

4.2.1. Initial electrical resistance

The nominal resistivity of the gold stripes was calculated as $\rho = R_{exp.}\frac{L}{Wh}$, where $R_{exp.}$ is the measured conductor resistance, L, W, and h the macroscopic length, width, and thickness, respectively. Samples prepared on glass slides were used

as reference. The electrical resistance of a 25-nm thick, 430-μm wide and 2.54-cm long stripe on glass is 142 Ω, which translates to a nominal resistivity of ~6 μΩ cm, which is two to three times that of bulk gold (2.3 μΩ cm).

The electrical resistivity of buckled stripes (on relaxed or pre-stretched substrate) lies in the range of that of stripes on glass. The electrical resistivity of the flat, micro-cracked, samples is higher, 3–40 times that of Au films evaporated on glass. In this case, the Au film can be described as a dense network of Au around voids. Its electrical conduction depends on the effective length and width of the gold conductor. Thus the initial electrical resistivity of the Au stripes depends on the substrate, the Au thickness, and the microstructure. The dependence of the electrical resistance on tensile strain differs between samples with the two surface morphologies.

4.2.2. *Electrical resistance during tensile deformation—substrates not pre-stretched*

We measured the electrical resistance of initially buckled and of initially flat samples under mechanical strain, up to electrical failure. Our definition of failure strain is the mechanical strain applied at the point of electrical failure. Most of the buckled samples show similar electro-mechanical behavior. As shown in Fig. 7 their electrical resistance linearly increases with the applied strain, reaches a critical strain above which the resistance dramatically jumps, and at a somewhat larger strain the sample fails. The value of the critical strain depends on the Au film thickness and its microstructure.

The resistance of initially micro-cracked samples is high, and increases steadily with the applied tensile strain. No macroscopic and negligible microscopic changes in the Au film was observed after tensile deformation up to 50% [23].

4.2.3. *Electrical resistance during tensile deformation—pre-stretched substrates*

Fig. 5 presents the electrical resistance of a 15% pre-stretched sample as a function of the applied strain, and photographs at 1%, 15%, and 28% tensile strain. When the substrate was stretched in the X direction beyond about 15%, the metal film came under tensile stress in the X direction, and under compressive stress in the Y direction. Consequently cracks formed normal to the X direction, and waves formed normal to the Y direction as shown on photograph taken at 28% in Fig. 5. The resistance in Fig. 5 exhibits two regimes. First it decreases with increasing strain ε up to 17%, i.e., beyond the value of the pre-stretch of 15%. At higher strain the resistance keeps increasing until it rises suddenly to open circuit at ~28% strain. The highest strain we have reached

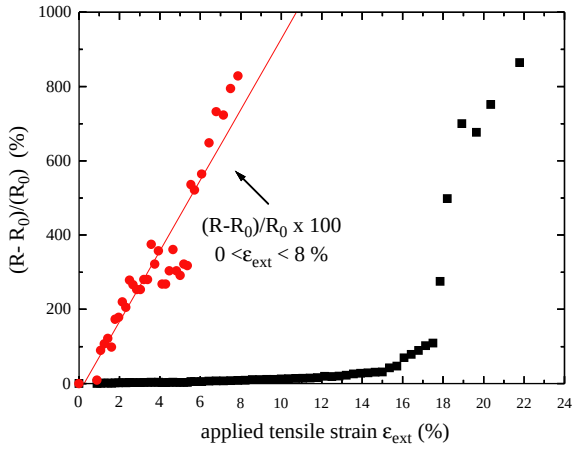

Fig. 7. Variation of the normalized electrical resistance $(R—R_0)/R_0$ of a 100-nm thick and 250-μm wide gold stripe with applied tensile strain ε_{ext} (in %).

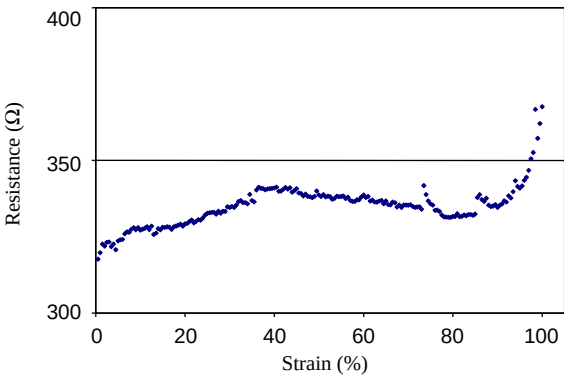

Fig. 8. Variation of the electrical resistance of a 3-mm wide, 2.5-cm long, 20-nm thick, gold stripe made on a 25% pre-stretched PDMS membrane. The sample showed low electrical resistance up to 100% stretch.

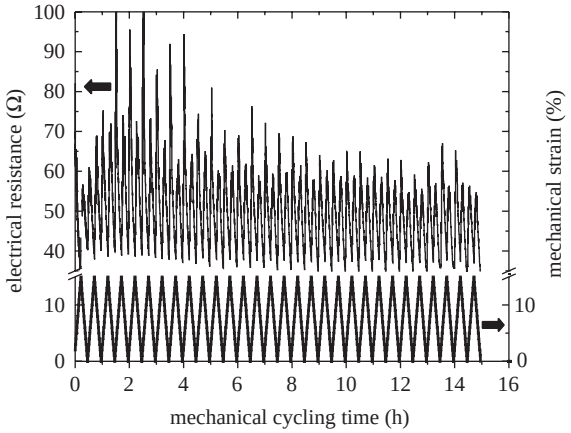

Fig. 9. Electrical resistance during mechanical cycling between 0% and 15% strain.

in Au stripes before electrical failure was 100% as demonstrated in Fig. 8. We have no evidence for plastic deformation of the PDMS substrate.

4.2.4. Mechanical cycling

Elastic interconnects may be cycled a few times (in shaping a conformal display or inserting a tracheal tube) to millions of times (in a polymer actuator). Fig. 9 shows the electrical resistance under cyclic strains between 0% and 15%, stepped by 1% every minute. The electrical resistance first stabilized and then settled between ~ 38 and $\sim 70\,\Omega$. In our longest tests the samples remained electrically stable through 200 cycles.

Thus gold stripes prepared on elastomeric membranes can function as interconnects for thin film transistor circuits on elastomeric substrates, as they meet input/output impedance requirements in the megaohm range, and can be deformed repeatedly.

A comparison of the resistance and strain traces of Fig. 9 shows that the electrical cycle is half as long as the mechanical cycle. The electrical resistance reaches its minimum at each of the minima and maxima of the mechanical strain; the resistance has maxima halfway through the mechanical extension or relaxation. We observed similar behavior in initially flat Au stripes [23].

5. Mechanical modeling

We are analyzing the mechanics of deformation and rupture of metal films bonded to the polymer substrate [10]. Our main concerns have been small deformation, large deformation, and conditions under which the metal film ruptures. Our idealized structure is a blanket metal film bonded to a polymer substrate, subject to a tensile strain in the plane of the film. Attention is restricted to metal films that rupture by strain localization (e.g., necking or forming a shear band). Strain localization causes a large local elongation in the metal film, which cannot be accommodated by the polymer substrate subject to a modest strain. One therefore expects that, when substrate-bonded and strain delocalized, the metal film may deform uniformly far beyond than its freestanding counterpart for which strain localization occurs (Fig. 10a). Of course, substrate constraint disappears if the metal film debonds from the polymer substrate. When the laminate is subject to a modest tensile strain, we expect strain localization and debond to co-evolve as depicted by Fig. 11. Without debonding, the polymer substrate suppresses strain localization in the

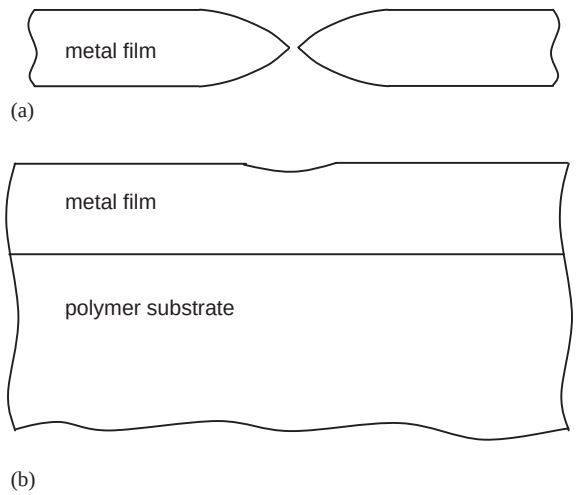

Fig. 10. When rupture is caused by strain localization, local thinning leads to local elongation. (a) For a free-standing metal film, the local elongation is accommodated by rigid body motion of the ruptured halves. (b) For a substrate-bonded film, the local elongation may be suppressed by the substrate.

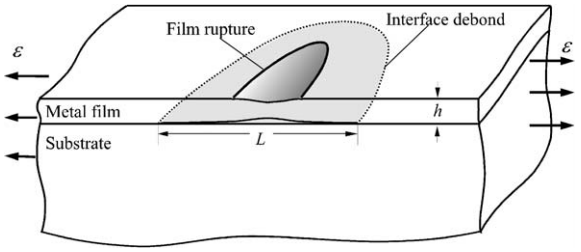

Fig. 11. A metal film is initially bonded to a thick polymer substrate. Subject to a tensile strain in the plane of the film, the film ruptures and the interface debonds simultaneously. The rupture occurs by localized strain in a segment of the film comparable to the film thickness, but debond spreads over a segment of the interface many times the film thickness.

metal. Without localization, no traction exists on the interface to drive debonding (Fig. 10b).

Incipient nonuniform deformation can be studied using a linear perturbation analysis. It shows that the substrate greatly elevates the applied strains needed for long wave perturbations to amplify [10]. The linear perturbation analysis, however, is invalid when the perturbation amplitude is comparable to the film thickness, or the perturbation wavelength, or the material inhomogeneity size. To address these concerns, we studied large-amplitude nonuniform deformation debond-assisted necking using the finite element method. One key result of our analysis is that the polymer substrate suppresses the necking of the film. This is shown schematically in Fig. 10b. Therefore, the film may rupture only at very high strain.

6. Conclusions and outlook

The successful fabrication of stretchable thin-film conductors has opened the door to making stretchable electronic surfaces. Much work remains to be done before stretchable conductors can be used as interconnects for skin-like circuits. Applied work will include techniques for micropatterning, simultaneous stretching of conductors running in both X and Y directions, and contacting membrane surfaces. And fundamental study is needed of the nature of bonding between the polymer substrate and the metal film, the effect of nucleation on built-in strain and initial microstructure, the mechanism underlying stretchability and of electrical conduction across fractures, and the mechanical mechanisms of electrical failure. We anticipate further discoveries of practical use and scientific interest.

Acknowledgements

This research was supported by the National Science Foundation, by DARPA, and by the New Jersey Commission on Science and Technology.

References

[1] V.J. Lumelsky, M.S. Shur, S. Wagner, IEEE Sensor J. 1 (2001) 41.
[2] Y. Bar-Cohen, SPIE, Bellingham, WA, 2001, pp. 671.
[3] S. Wagner, E. Bonderover, W.B. Jordan, J.C. Sturm, Int. J. High Speed Electron. Systems 12 (2002) 1.
[4] P.-H. Hsu, R. Bhattacharya, H. Gleskova, Z. Xi, Z. Suo, S. Wagner, J.C. Sturm, Appl. Phys. Lett. 81 (2002) 1723.
[5] E. Bonderover, S. Wagner, Z. Suo, Mater. Res. Soc. Symp. Proc. 769 (2003) H9.
[6] H. Gleskova, S. Wagner, W. Soboyejo, Z. Suo, J. Appl. Phys. 92 (2002) 6224.
[7] D.W. Pashley, Proc. R. Soc. London A 255 (1960) 218.
[8] H. Huang, F. Spaepen, Acta Mater. 48 (2000) 3261.
[9] H.D. Merchant, J.T. Wang, L.A. Giannuzzi, Y.L. Liu, Circuit World 26 (4) (2000) 7.
[10] T. Li, Z.Y. Huang, Z.C. Xi, S.P. Lacour, S. Wagner, Z. Suo, Mechanics of Materials, in press.
[11] R.R. Bhattacharya, S. Wagner, Mater. Res. Soc. Symp. Proc. 769 (2003) H10.5.
[12] G.C. Martin, T.T. Su, I.H. Loh, E. Balizer, S.T. Kowel, P. Kornreich, J. Appl. Phys. 53 (1982) 797.
[13] W.T.S. Huck, N. Bowden, P. Onck, T. Pardoen, J. Hutchinson, G.M. Whitesides, Langmuir 16 (2000) 3497.
[14] S.P. Lacour, S. Wagner, Z. Huang, Z. Suo, Appl. Phys. Lett. 82 (2003) 2404.
[15] M. Maghribi, J. Hamilton, D. Polla, K. Rose, T. Wilson, P. Krulevitch, in: Proceedings of the Second Annual International IEEE-EMBS Special Topic Conference on Microtechnologies in Medicine & Biology, 2002, pp. 80.
[16] A.L. Volynskii, S. Bazhenov, O.V. Lebedeva, N.F. Bakeev, J. Mater. Sci. 35 (2000) 547.
[17] M. Watanabe, H. Shirai, T. Hirai, J. Appl. Phys. 92 (2002) 4631.
[18] R. Abermann, R. Koch, Thin Solid Films 129 (1985) 71.

[19] J.A. Floro, S.J. Hearne, J.A. Hunter, P. Kotula, E. Chason, S.C. Seel, C.V. Thompson, J. Appl. Phys. 89 (2001) 4886.
[20] S.P. Lacour, S. Wagner, Z. Huang, Z. Suo, Mater. Res. Soc. Proc. 736 (2002) D4.8.1.
[21] J. Jones, S.P. Lacour, Z. Suo, S. Wagner, Mater. Res. Soc. Proc. 769 (2003) H.6.12.1.
[22] S.P. Lacour, J. Jones, Z. Suo, S. Wagner, IEEE Electron Device Lett. 25 (2004) 179.
[23] C. Chambers, S.P. Lacour, Z. Suo, S. Wagner, Z. Huang, Mater. Res. Soc. Proc. 769 (2003) H10.3.1.